Processing and Characterization of Porous Structures from Chitosan and Starch for Tissue Engineering Scaffolds

Javier Nakamatsu,[†] Fernando G. Torres,*[,†] Omar P. Troncoso,[†] Yuan Min-Lin,[‡] and Aldo R. Boccaccini*[,‡]

Polymers and Composites Group, Catholic University of Peru, Lima 32, Peru, and Department of Materials and Centre for Tissue Engineering and Regenerative Medicine, Imperial College London, London SW7 2BP, UK

Received June 2, 2006; Revised Manuscript Received September 22, 2006

Natural biodegradable polymers were processed by different techniques for the production of porous structures for tissue engineering scaffolds. Potato, corn, and sweet potato starches and chitosan, as well as blends of these, were characterized and used in the experiments. The techniques used to produce the porous structures included a novel solvent-exchange phase separation technique and the well-established thermally induced phase separation method. Characterization of the open pore structures was performed by measuring pore size distribution, density, and porosity of the samples. A wide range of pore structures ranging from 1 to 400 μm were obtained. The mechanisms of pore formation are discussed for starch and chitosan scaffolds. Pore morphology in starch scaffolds seemed to be determined by the initial freezing temperature/freezing rate, whereas in chitosan scaffolds the shape and size of pores may have been determined by the processing route used. The mechanical properties of the scaffolds were assessed by indentation tests, showing that the indentation collapse strength depends on the pore geometry and the material type. Bioactivity and degradation of the potential scaffolds were assessed by immersion in simulated body fluid.

1. Introduction

Tissue engineering (TE) offers an alternative approach to the repair and regeneration of damaged human tissue.[1] Different strategies are available for the regeneration of tissues, such as cell infiltration, tissue cultivation on porous scaffolds, 3-D cell printing, and injectable scaffolds. The development of porous scaffolds is one of the most challenging and interesting techniques in tissue engineering.[1−4] Exploiting suitable cells−scaffold interactions, tissues can be generated in vitro and then implanted in the human body, where required.

For the proper attachment and proliferation of cells of a particular tissue in these porous scaffolds, adequate manufacturing techniques must be developed, which should allow for proper control of the levels of porosity, pore shape distribution, and pore interconnectivity.[2] These physical properties must be tailored to fulfill the requirements of the particular tissue under consideration to provide mechanical stability and space for expansion and allow the diffusion of oxygen and nutrients, waste clearance, invasion of blood vessels, and building of tissue layers.[5]

Moreover, scaffold materials should be tested for biocompatibility and biodegradation or bioresorption. In the past, mostly synthetic biodegradable polymers such as polycaprolactone (PCL) and polylactic acid (PLA) have been used for the production of polymeric scaffolds.[1,2] More recently, studies have also focused on the use of natural biodegradable materials for tissue engineering scaffolds.[3]

Research has been for example carried out on starch.[6] Starch is a polymer composed of anhydroglucose units, which occurs widely in plants. Native starch granules are composed of two major polymers: Amylose and amylopectin (Figure 1). Amylose is essentially linear (α-1→4-linked glucose unit) while amylopectin is branched (α-1→4-linked glucose unit interlinked by α-1→6-D-glucosidic linkage) and makes up about 80% of the granule. The solubility of starch granules depends mainly on the amylose content as this component has been shown to be solubilized.[7,8] In contrast, the semicrystallinity of starch granules, which gives rise to the Maltese cross observed under polarized light (see Figure 3), is due to the amylopectin.[9]

Gomes et al.[6] have compared different processing techniques for the production of scaffolds based on commercial thermoplastic corn starch. Among the processing techniques reported in their study are extrusion with blowing agents, compression molding with particulate leaching, solvent casting with particulate leaching, and in situ polymerization.

Chitosan is a linear copolymer of glucosamine and *N*-acetyl glucosamine units linked by β-1→4-bonds (Figure 2). Chitosan is the partially deacetylated form of chitin, a widespread natural polysaccharide. Due to its characteristics, chitosan has been extensively studied for a broad variety of applications from wastewater treatment and agriculture to cosmetics and pharmaceutics. Among the potential uses of chitosan, tissue engineering has attracted increased attention in the past decade due to the material's biocompatibility,[10−12] its intrinsic antibacterial and antifungal activity,[13] bioresorption,[14] and its biodegradability.[15] In contrast to chitin, chitosan is soluble, which makes it easy to process and purify; its film and fiber forming abilities have been studied. Chitosan is suitable for tissue regeneration scaffolds when it is formed into highly porous structures.[16] It is not cytotoxic to fibroblasts and allows for the formation of bioactive Ca−P layers on its surface when exposed to simulated body fluid.[17] Chitosan, in its linear or cross-linked form, has also been combined with other materials such as gelatin,[18−20] alginate,[21,22]

* Correspondong authors. E-mail: fgtorres@pucp.edu.pe; a.boccaccini@imperial.ac.uk.

[†] Catholic University of Peru.

[‡] Imperial College London.

10.1021/bm0605311 CCC: $33.50
Published on Web 11/14/2006

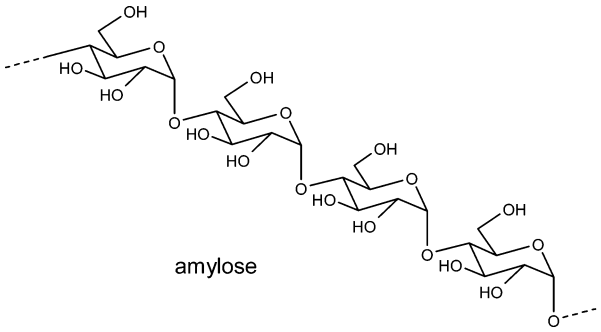

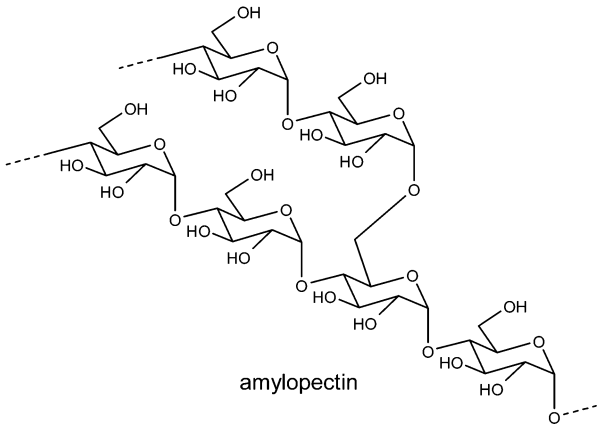

Figure 1. Components of starch, linear amylose, and branched amylopectin.

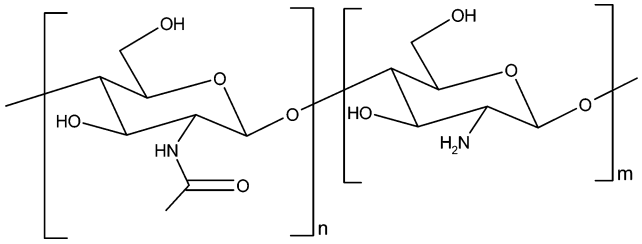

Figure 2. Chitosan structure showing glucosamine and *N*-acetyl glucosamine units.

poly(lactic acid), collagen,[23,24] calcium phosphate,[25,26] hyaluronic acid,[27] peptides,[28] and hydroxyapatite.[29] The scaffolds produced have been studied for tissue repair (cartilage, bone, skin, and disks).[30]

The preparation of water-soluble chitin and chitosan derivatives has been revised by Sugimoto et al.[31] Chow and Khor[32] developed a technique for the production of open pore chitin matrixes, based on the leaching of calcium carbonate particles. They were able to produce structures with homogeneous pores in the range 100−1000 μm corresponding to porosities between 76% and 81%. Fernandez-Cervera et al.[33] recently produced films of binary mixtures of chitosan and amylose corn starch using the casting/solvent evaporation method. Glycerol, sorbitol, and i-erythritol were used as plasticizers. Previously, Arvanitoyannis et al.[34] had produced chitosan−PVA blends plasticized with sorbitol and sucrose. Films of chitosan and PEO have been prepared by Budtova et al.[35] and their rheological, transport, and mechanical properties were characterized.

The objective of the present research is to develop scaffolds with controlled porosity for applications in tissue engineering using chitin, chitosan, and starch. These natural polymers and their blends were compared in terms of their processability, mechanical properties, and biodegradability. The manufacturing techniques used were thermally induced phase separation and freeze-drying. Pore size distributions, density, porosity, and indentation stress were measured to characterize the scaffolds produced. Control of porosity and pore interconnectivity are key issues to be addressed when assessing processability. The investigations represent a novel contribution toward the development of tailored porous structures showing a wide range of pore sizes and shapes, produced under a wide variety of controlled processing routes, not reported previously for the materials described here.

2. Experimental Section

2.1. Materials. Chitosan was provided by IDEBIO in scale form with a characteristic dimension of about 1 mm. It was obtained from centollon, a crab species from the southern part of South America. The sample had a molecular weight of 860000 Da, measured by viscosity, and a degree of deacetylation of 88% (determined by infrared spectroscopy).

The degree of deacetylation of chitosan was determined by IR spectroscopy from films. Films were prepared from CH_3CO_2H 1% (v/v) solutions, air-dried, and then washed with NH_3-CH_3OH (1:7 mixture) and pure CH_3OH. The percentage of *N*-acetyl groups was calculated from the absorption bands at 1655 and 3450 cm^{-1}, according to the literature.[36]

Molecular weight of chitosan was determined by intrinsic viscosity of the solution in a 0.1 M $CH_3CO_2Na-0.2$ M CH_3CO_2H buffer at 30 °C, using an Ubbelohde viscometer. Mark−Houwink constants ($\alpha = 0.96$ and $K = 1.424 \times 10^{-3}$ mL/g) were taken from the literature.[37]

Potato, corn, and sweet potato starch of an industrial food grade (NEGRITA) was used. Starch granules were observed under polarized light and particle shape and dimensions were recorded (Figure 3). The oval shape and particle size (50−100 μm) of potato starch granules, as well as the Maltese cross pattern observed under polarized light, are in agreement with observations reported elsewhere.[9,38] Water, glycerol, ethylene glycol, and propylene glycol were used as plasticizers[39−41] in concentrations up to 10% by weight.

The simulated body fluid (SBF) used to test the in vitro bioactivity of scaffolds was prepared by dissolving corresponding amounts of reagent chemicals (all purchased from Sigma, Steinheim, Germany) NaCl, $NaHCO_3$, KCl, $K_2HPO_4 \cdot 3H_2O$, $MgCl_2 \cdot 6H_2O$, $CaCl_2 \cdot 2H_2O$, and Na_2SO_4 into distilled water. The SBF was adjusted to physiological pH (pH 7.25) with HCl and buffered by tris(hydroxyl-methyl) aminomethane.

2.2. Preparation of the Specimens: Specific Processing Routes. *2.2.1. Starch Samples.* Samples were prepared by mixing potato, corn, or sweet potato starch with distilled water in different concentrations, ranging from 10 to 20% (w/w) (see Table 1). The starch suspension was stirred and heated in a water bath (at 70 °C) until a homogeneous paste was formed. The paste was transferred into plastic moulds and allowed to reach room temperature. Samples were frozen in liquid nitrogen (−196 °C) or in a freezer (−15 °C). These samples were then either freeze-dried in a Labconco Freeze Dry System (pressure = 0.13 mbar) or immersed in ethanol at −15 °C and allowed to reach room temperature. In the latter case, the samples were washed with more ethanol at room temperature and then allowed to dry under airflow. Samples were finally dried under vacuum. A summary of the processing routes for the different starch compositions is given in Figure 4.

2.2.2. SEPS Chitosan Samples. A solution of 1.45 g of chitosan in 60 mL of diluted acetic acid (1% v/v) was prepared by stirring the mixture for 6 h at room temperature; the solution was then filtered through a glass filter to remove insoluble particles. Portions of this chitosan solution were processed in four different ways: Degassed and non-degassed specimens frozen at −15 and −196 °C.

The portion of the solution degassed was introduced into the vacuum chamber before freezing. Freezing was performed either in a freezer (−15 °C) or in liquid nitrogen (−196 °C). Samples frozen in liquid

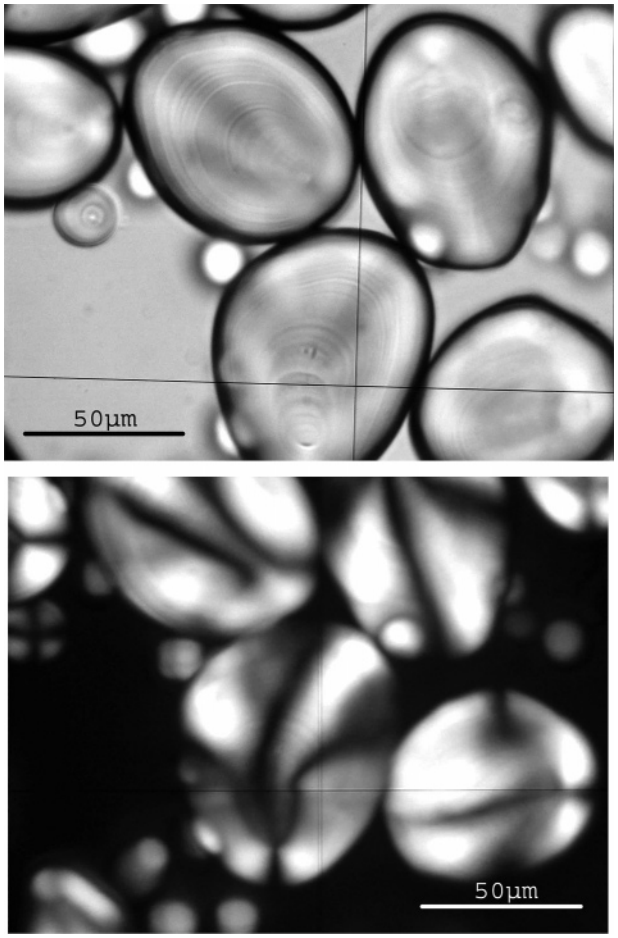

Figure 3. Potato starch granules. Top: without polarized light. Bottom: with polarized light, showing the typical Maltese cross structure of starch.

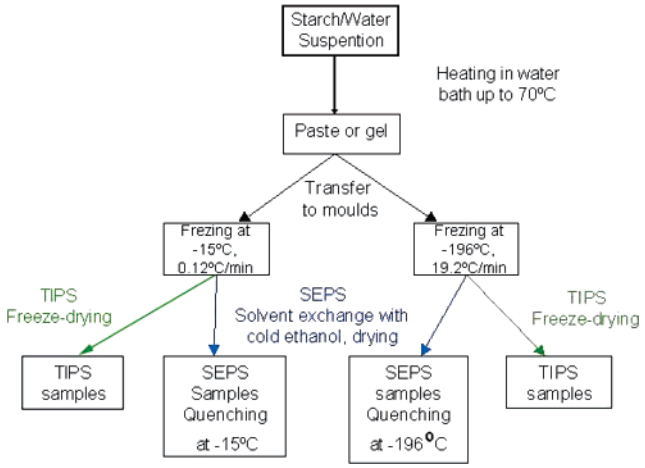

Figure 4. Processing routes used for the preparation of scaffolds with all the different starch compositions.

nitrogen were then kept in the freezer (−15 °C) until the next step. All frozen samples were then immersed in a mixture of methanol and concentrated aqueous ammonia (7:3 in volume) previously cooled to −15 °C and left at this temperature overnight. The samples in the basic solution were allowed to reach room temperature and then they were taken out of the basic solution and rinsed with methanol until neutral pH. Finally, the samples were rinsed with acetone several times to exchange solvents and were allowed to dry under vacuum at room temperature.

2.2.3. Precipitated Chitosan Samples. Chitosan (1.51 g) was dissolved in 50 mL of diluted acetic acid (1% v/v) as mentioned above. The solution was precipitated dropwise in 500 mL of an alkaline solution made of ethanol (60 mL) and 0.7 M $NaOH_{(aq)}$ (440 mL) with gentle stirring. Pellet-like foams were formed, with diameters around 3.5 mm (depending on drop size), and left in the solution for 10 h at room temperature. The samples were then washed with distilled water several times until neutral pH was reached. Final rinsing was performed

Table 1. Starch Specimens Preparation

starch sample	starch source	concentration % (w/w)	freezing temperature (˚C)	process
ST-P-10-15-SX	potato	10	−15 ˚C	solvent exchange
ST-P-10-15/N-FD	potato	10	−15 ˚C	freeze-dry
ST-P-10-N-FD	potato	10	−196 ˚C	freeze-dry
ST-P-10-N-SX	potato	10	−196 ˚C	solvent exchange
ST-P-20-15-SX	potato	20	−15 ˚C	solvent exchange
ST-P-20-15/N-FD	potato	20	−15 ˚C	freeze-dry
ST-P-20-N-FD	potato	20	−196 ˚C	freeze-dry
ST-P-20-N-SX	potato	20	−196 ˚C	solvent exchange
ST-C-10-15-SX	corn	10	−15 ˚C	solvent exchange
ST-C-10-15/N-FD	corn	10	−15 ˚C	freeze-dry
ST-C-10-N-FD	corn	10	−196 ˚C	freeze-dry
ST-C-10-N-SX	corn	10	−196 ˚C	solvent exchange
ST-C-20-15-SX	corn	20	−15 ˚C	solvent exchange
ST-C-20-15/N-FD	corn	20	−15 ˚C	freeze-dry
ST-C-20-N-FD	corn	20	−196 ˚C	freeze-dry
ST-C-20-N-SX	corn	20	−196 ˚C	solvent exchange
ST-SP-10-15-SX	sweet potato	10	−15 ˚C	solvent exchange
ST-SP-10-15/N-FD	sweet potato	10	−15 ˚C	freeze-dry
ST-SP-10-N-FD	sweet potato	10	−196 ˚C	freeze-dry
ST-SP-10-N-SX	sweet potato	10	−196 ˚C	solvent exchange
ST-SP-20-15-SX	sweet potato	20	−15 ˚C	solvent exchange
ST-SP-20-15/N-FD	sweet potato	20	−15 ˚C	freeze-dry
ST-SP-20-N-FD	sweet potato	20	−196 ˚C	freeze-dry
ST-SP-20-N-SX	sweet potato	20	−196 ˚C	solvent exchange

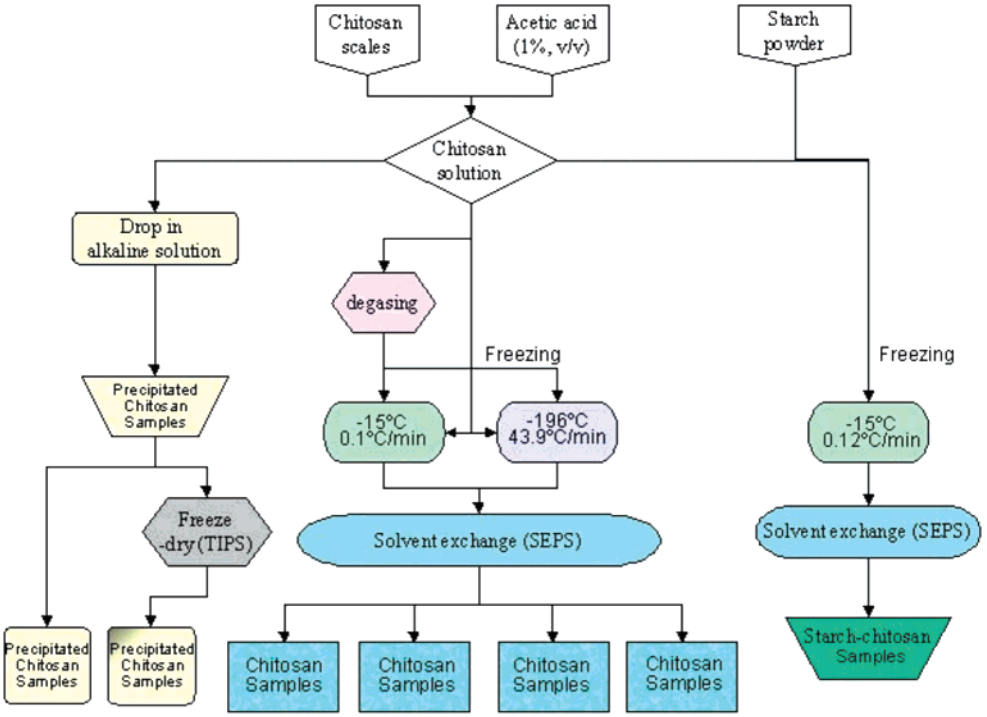

Figure 5. Processing routes used for the preparation of chitosan and chitosan−starch scaffolds.

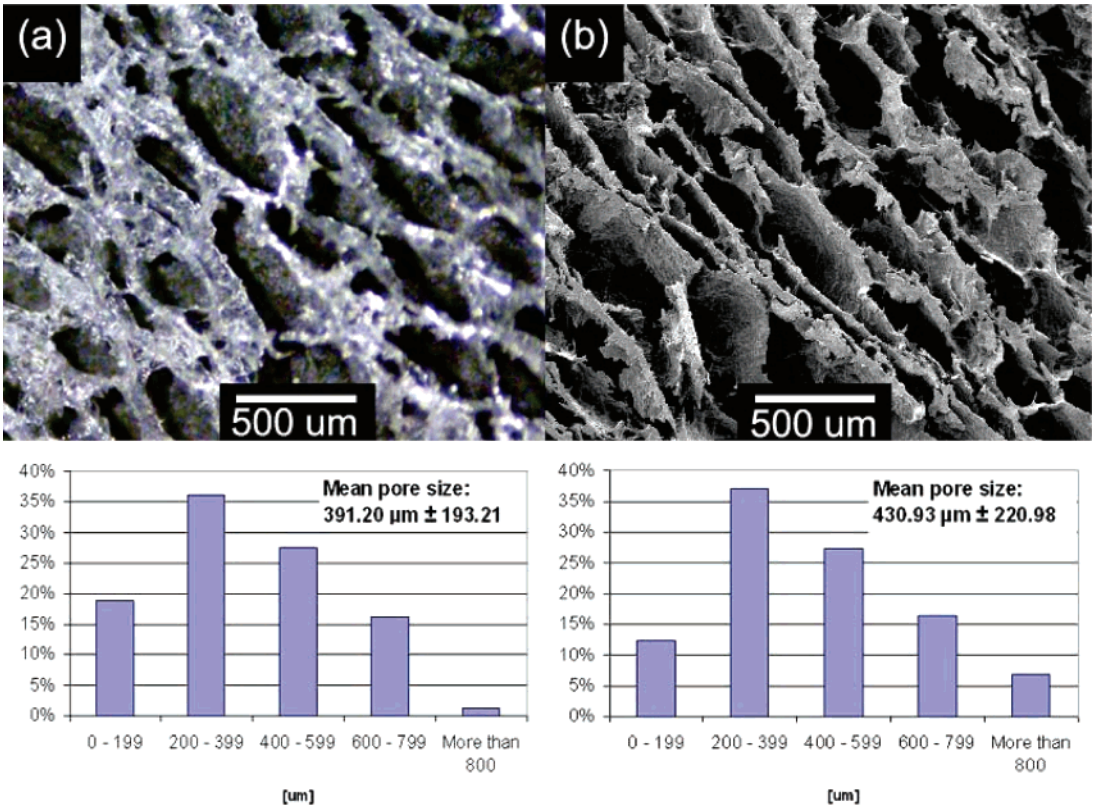

Figure 6. (a) LOM micrograph of specimen ST-SP-10-15-SX (sweet potato scaffold), (b) SEM micrograph of specimen ST-SP-10-15-SX (sweet potato scaffold).

with 100 mL of distilled water at 75 °C. A portion of these was freeze-dried and the other portion was dried at room temperature with airflow and then under vacuum.

2.2.4. Starch−Chitosan Samples. Potato starch (8.63 g) was suspended in 50 mL of a 1% (w/w) chitosan solution in acetic acid (1% v/v). The suspension was stirred for 3 h, and then it was heated in a water bath (70 °C) until a paste was formed. The paste was transferred to a plastic mould and frozen at −15 °C overnight. The frozen sample was then immersed in a 1% solution of ammonia in ethanol (v/v) at −15 °C for 4 h and then allowed to reach room temperature. The sample (ST−CH) was then washed with more ethanol until neutral pH and then dried under vacuum.

A summary of the processing routes for chitosan and chitosan−starch blends is given in Figure 5.

2.3. Morphological Characterization. Polarized light optical microscopy (PLOM) was used to characterize the structure of starch

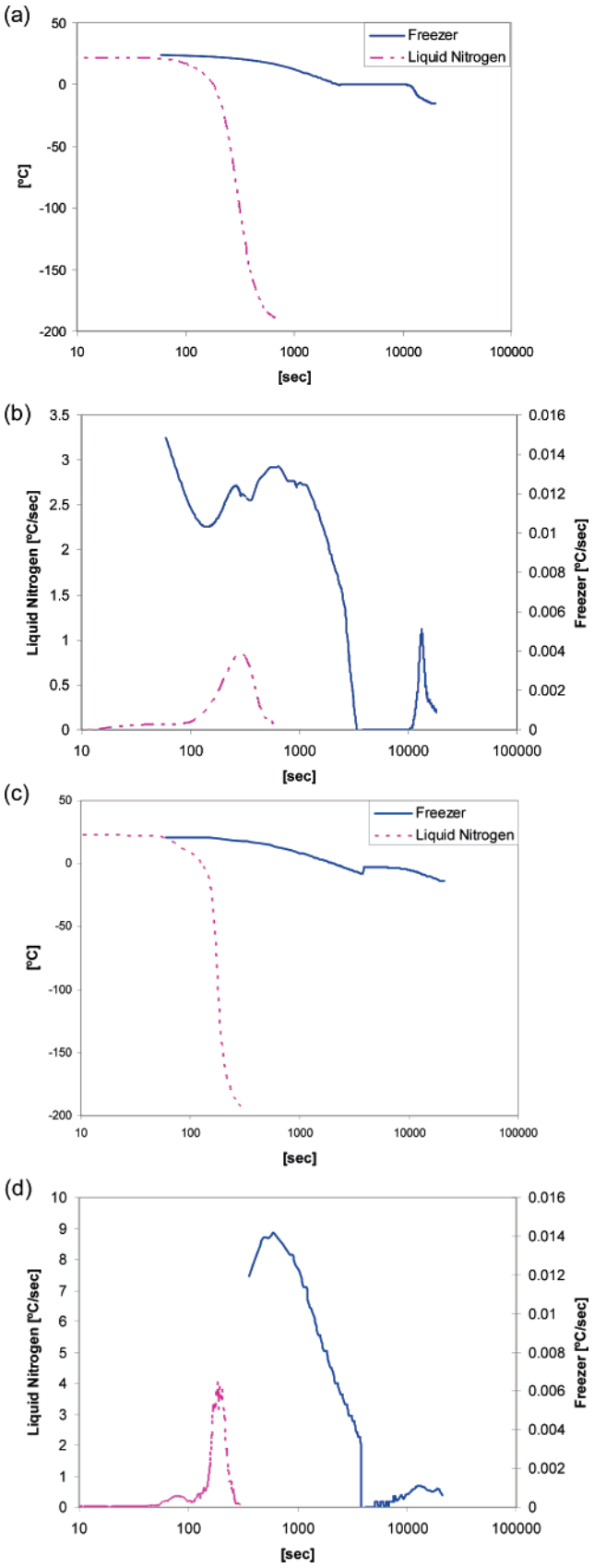

Figure 7. (a) Variation of temperature with time for specimen ST-P-20 (potato scaffold), (b) instantaneous freezing rate as a function of time for specimen ST-P-20, (c) variation of temperature with time for a SEPS chitosan sample, and (d) instantaneous freezing rate as a function of time for a SEPS chitosan sample.

granules. Stereomicroscopy using a BRUNEL BMZ trinocular stereomicroscope was used to characterize features at the mesoscale[42,43] since it offers an adequate magnification and depth of field for studies at the mesoscale.

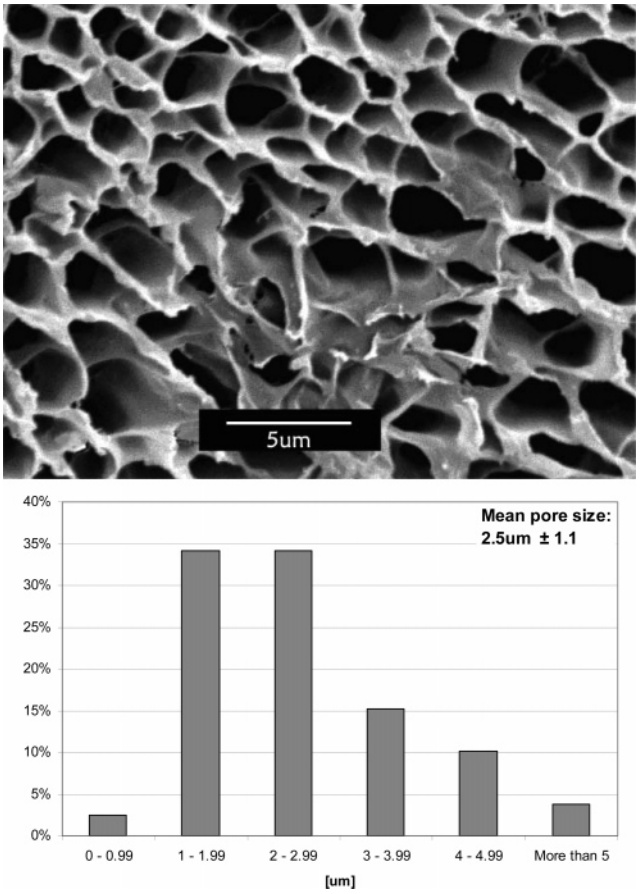

Figure 8. SEM micrograph and pore size distribution of a potato starch scaffold (ST-P-20-N-FD) frozen at −196 °C and produced by thermally induced phase separation (TIPS) showing microporous isotropic structure.

Table 2. Type of Foams for Different Materials Manufacturing Processes

source	freezing temperature (°C)	process	type of foam
starch	−15	solvent exchange	macroporous
	−15	freeze-dry	macroporous
	−196	solvent exchange	microporous
	−196	freeze-dry	microporous
chitosan	−15	solvent exchange	macroporous
	−196	solvent exchange	macroporous
		chitosan precipitation	microporous
starch/chitosan	−15	solvent exchange	macroporous

Surface and pore morphology and specimen microstructure homogeneity were assessed using scanning electron microscopy (SEM) (JEOL JSM). Small pieces of the specimens were mounted onto stubs using adhesive tapes and sputtered with a gold layer. Accelerating voltages in the range of 6−18 kV were used for the observation of cross sections and surface topography.

Image analysis of the SEM micrographs was performed using the ImageJ software developed at the Research Services Branch (RSB) of the National Institute of Mental Health (NIMH), part of the National Institutes of Health (NIH) of the USA. The maximum Feret Diameter (i.e., the maximum distance between parallel lines tangent to the pore profile) was used to characterize the pore size.[44]

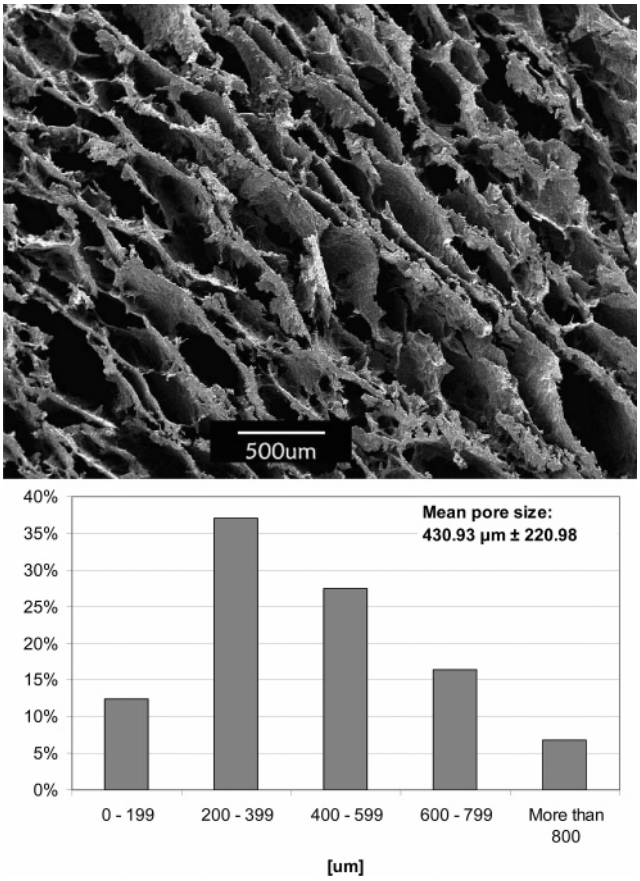

Figure 9. SEM micrograph and pore size distribution of a sweet potato starch scaffold (ST-SP-10-15-SX) frozen at −15 °C and produced by solvent exchange phase separation (SEPS) showing macroporous anisotropic structure.

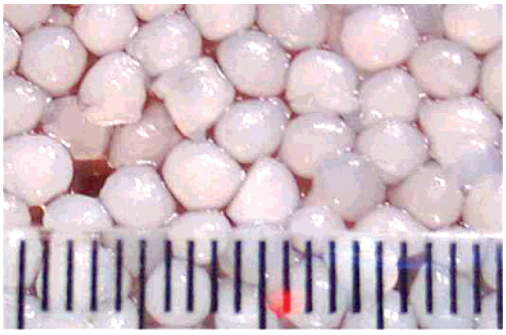

Figure 10. Microporous freeze-dried chitosan pellets in the wet state (each division corresponds to 1 mm).

2.4. Freezing Rate. The freezing rates of chitosan, starch, and starch/chitosan samples both in a freezer (−15 °C) and in liquid nitrogen were measured using a K type thermocouple and a Tokio Sokki Kenkyujo TC-31K data logger with a resolution of 0.1 °C and a sampling speed of 0.5 s.

2.5. Density and Porosity Estimates. The volume and mass of cubic foam specimens (nominally 5 × 5 × 5 mm^3) were determined. Measurements of the overall dimensions were taken using vernier callipers (across 5 samples per composition). With use of the densities of the solid polymers, as is usual for TE scaffolds,[45−47] a theoretical porosity (P) was calculated based on a comparison of its apparent density to the bulk system according to eq 1,

$$P = 1 - \frac{\rho}{\rho_o} \quad (1)$$

where ρ is the foam density and ρ_o is the density of the nonporous material.

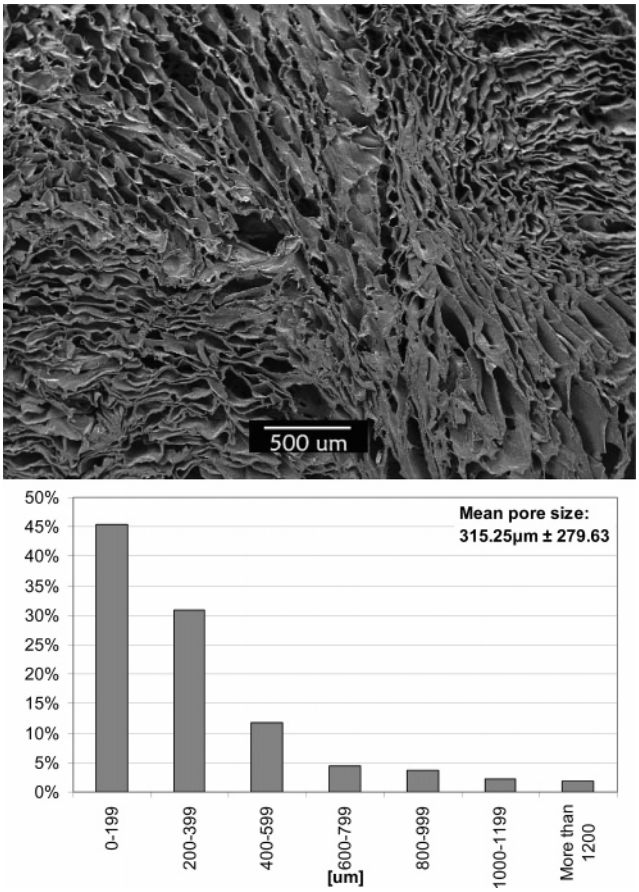

Figure 11. SEM micrograph and pore size distribution of a chitosan scaffold (not degassed) frozen at −196 °C and produced by solvent exchange phase separation (SEPS) showing macroporous anisotropic structure.

2.6. Bioactivity Tests in Simulated Body Fluid. In vitro bioactivity studies were carried out using a cellular simulated body fluid (SBF) based on the formulation and method developed by Kokubo et al.[48] After solvent evaporation overnight, the specimens attached to the cover glass were placed in 24-well plates using tweezers, and subsequently a 2 mL aliquot of SBF (37.8 °C) was added to the specimens. During the immersion period, the specimens were kept at 37.8 °C in a humidified incubator, and the SBF was refreshed after 6 h of incubation followed by 24 and 48 h and then every 3 days. Specimens were then collected after 1, 3, 7, 14, and 21 days of incubation. The samples were rinsed in distilled water three times, then vacuum-dried for 3 h, and finally stored in desiccators for further examination.

2.7. Indentation Test. Indentation tests were carried out using a DO-type durometer according to ASTM D2240.[49] An indenter with diameter of 2.38 mm was used. ASTM D2240 is prescribed for the determination of hardness of soft materials, such as rubbers, cellular plastics, and gel-like materials. The stress needed to produce a 1 mm indentation in the specimens was recorded. Three repeats were carried out for each sample.

3. Results and Discussion

3.1. Manufacturing Processes and Pore Morphology. The control of the pore size is achieved by the different processing routes. Pore size was estimated by image analysis as described in section 2.3. The error on pore size measurements due to the dehydration (≈10%) caused by the preparation of the samples for the SEM was estimated by comparing some SEM and light optical microscopy (LOM) pictures. In Figure 6, the two micrographs obtained from the same specimen show that a difference

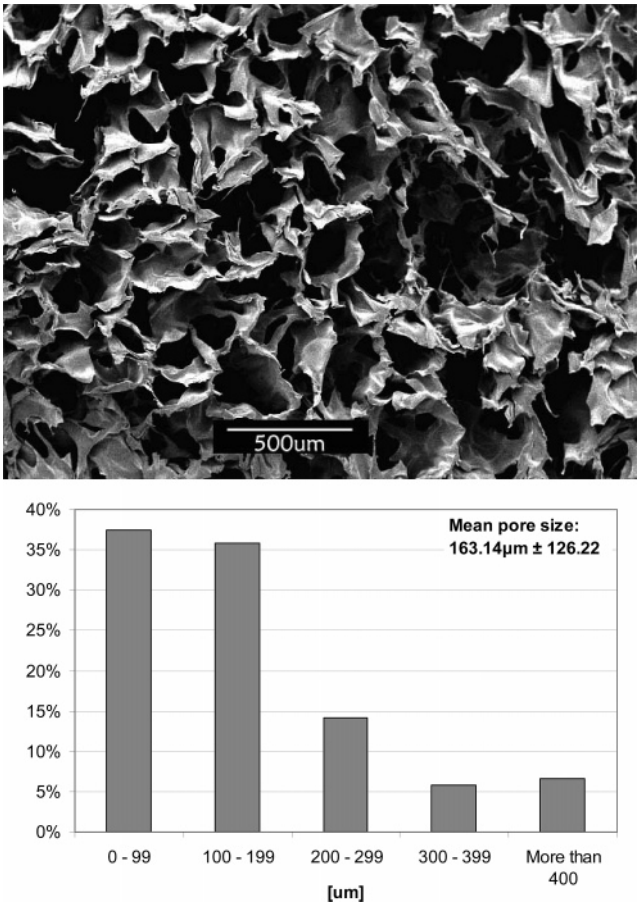

Figure 12. SEM micrograph and pore size distribution of a chitosan scaffold (degassed) frozen at −15 °C and produced by solvent exchange phase separation (SEPS) showing macroporous anisotropic structure.

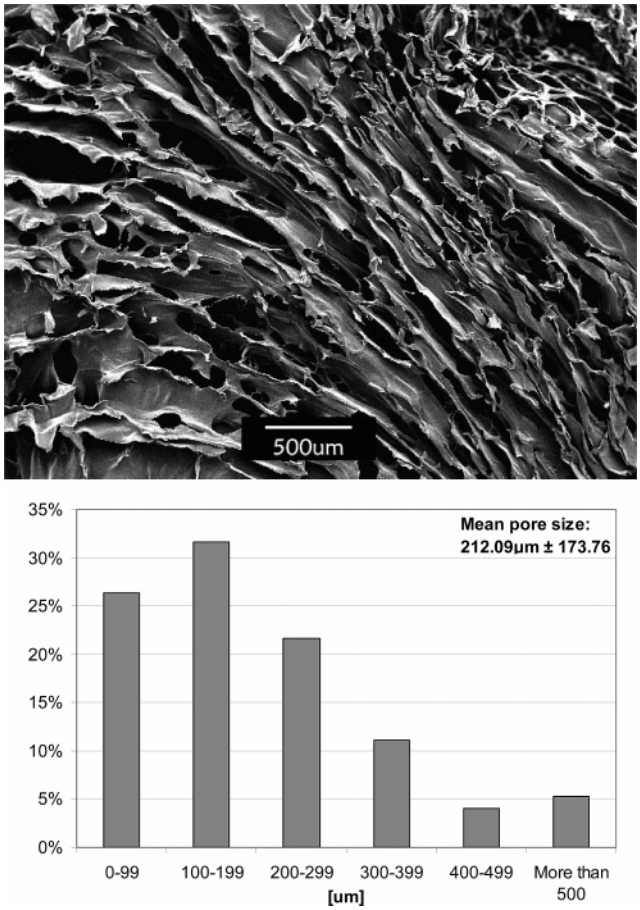

Figure 13. SEM micrograph and pore size distribution of a chitosan scaffold (degassed) frozen at −196 °C and produced by solvent exchange phase separation (SEPS) showing macroporous anisotropic structure.

of around 10% in the mean pore size measured with LOM and SEM can be observed. An error of such order of magnitude can be due to dehydration since the moisture content of the scaffolds at room conditions was in the range 5−7%.

Starch in water formed a milky white suspension. When heated in a water bath, starch underwent gelatinization. Thus, the granules swelled, absorbed water, and leached linear amylose chains.[9] The remaining granules had a higher concentration of amylopectin. Therefore, the starch paste produced can be idealized as a phased-separated system in which amylopectin-enriched granules are in a matrix of amylose molecules.[50] In this system, the glass transition temperature (T_g) is below the freezing temperature of water. Thus, during the cooling process, the ice formation starts before the paste reaches T_g (ca. −5 °C)[51] and the system will be separated into an ice phase and a non-vitreous polymer phase. The starch matrix increases its concentration as temperature decreases and more ice is formed until it solidifies into the glassy state and ice formation ceases.[52]

For starch-based scaffolds, the different routes produced either macroporous or microporous foams. Table 2 shows that it is not the water removal technique by solvent exchange (SEPS) or freeze-drying (TIPS) that determines the pore size of the foams but the freezing temperature of the starch−water paste (see Figure 4).

Figure 7 shows the two different freezing processes. When the samples were frozen in a commercial freezer, about 5 h was needed to reach the minimum temperature (−15 °C) at an average freezing rate of 0.002 °C/s (0.12 °C/min). By contrast, with liquid nitrogen, only 11 min was needed for the samples to reach −190 °C at an average freezing rate of 0.36 °C/s (19.2 °C/min). At the low freezing rate (freezer) the samples showed a typical freezing curve where a plateau is reached at 0 °C while phase changes take place and ice formation (nucleation) begins. On the other hand, samples frozen in liquid nitrogen showed a different type of freezing behavior without a plateau. At higher freezing rates, specimens might have the chance for a larger number of smaller crystals to develop.

For starch-based scaffolds, the type of foam obtained (macro- or microporous foam) depends on the physics of water freezing. When the samples were frozen in liquid nitrogen (−196 °C), the high freezing rate (19.2 °C/min) produced small ice crystals and then micropores (2.5 μm, Figure 8) while macropores (430.93 μm) were formed in a freezer at −15 °C (Figure 9) using a lower freezing rate (0.12 °C/min). This is in agreement with observations reported elsewhere.[53]

Chitosan is soluble in dilute acidic solutions such as 1% (v/v) aqueous acetic acid due to protonation of the free amine groups. When the solution is neutralized with NaOH or NH_3, chitosan precipitates. Precipitated and then freeze-dried chitosan samples maintain their size (Figure 10), whereas precipitated but non-freeze-dried samples (swollen state) shrink considerably to about 1 mm in diameter.

Drying of precipitated chitosan or any wet chitosan sample at ambient conditions results in shrinking due to interactions between polymers chains, especially due to the formation of strong hydrogen bonding from hydroxyl and amino groups as liquid water evaporates. On the other hand, when samples are freezed-dried, movement of polymer chains is highly restricted

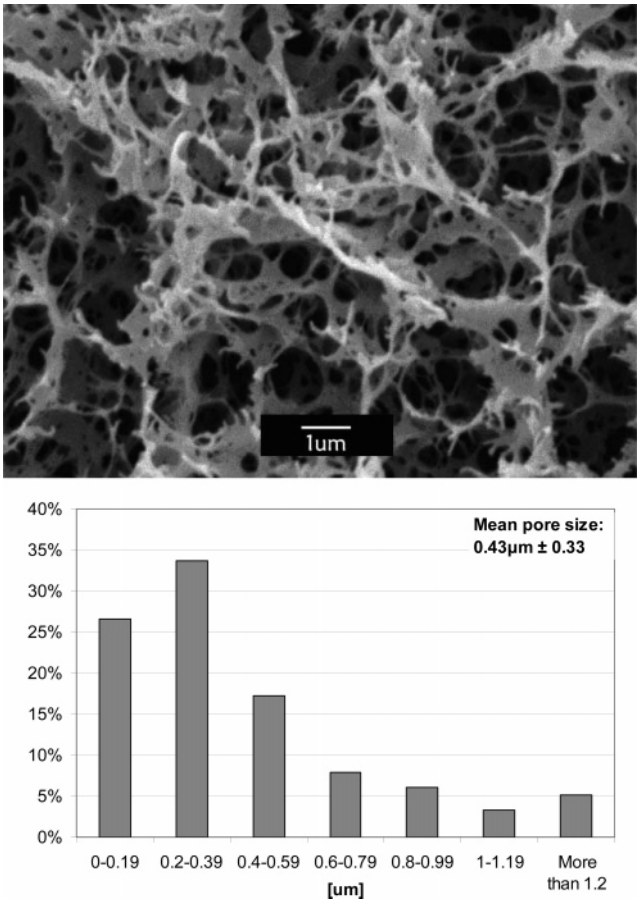

Figure 14. SEM micrograph and pore size distribution of a chitosan scaffold produced by thermally induced phase separation (TIPS) showing micro- and nanoporous isotropic structure.

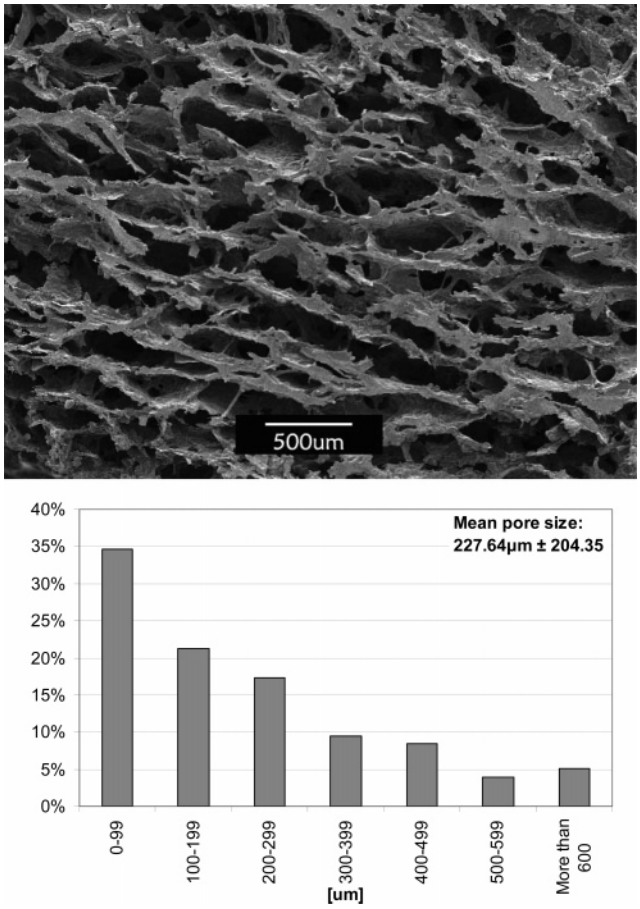

Figure 15. SEM micrograph and pore size distribution of a potato starch−chitosan blend frozen at −15 °C and produced by solvent exchange phase separation (SEPS) showing macroporous anisotropic structure.

since the entire sample is in the solid state (both polymer chains and water molecules). Thus, as water molecules are removed by sublimation, the polymer chains cannot move and remain in the same conformation (which results in no or reduced shrinkage).

For chitosan-based scaffolds, when using the solvent exchange technique (SEPS), only macroporous foams (≈163−315 μm, Figures 11−13) were obtained (see Table 2) regardless of the freezing temperature of the process. This could be due to the fact that the very low concentration of chitosan in water (≈2%) cannot affect the ice formation mechanism. Thus, all such samples have similar mean pore size values. However, microporous chitosan structures (0.43 μm, Figure 14) can be produced when the chitosan solution is first precipitated in an alkaline medium and then freeze-dried. In this case, precipitation of the polymer matrix is the main foaming mechanism rather than ice formation.

These micro- and nanoporous structures are not suitable for tissue engineering because pores are too small to allow cell growth and proliferation.[1,2] An alternative combined manufacturing process based on the techniques presented here should produce macro- and microporous structures that would be suitable for tissue engineering applications. The micro- and nanoporous scaffolds presented here (Figures 9 and 14) might, however, be suitable for the controlled delivery of drugs and agrochemicals.

The morphology of chitosan-based scaffolds (SEPS) is shown in Figures 11−13. All samples had an open and well-structured porous network. A tubular shape and orientated porous arrangement can be seen.

Degassing is important for chitosan foams since air is introduced when preparing the solution from the powdered form and during filtration. Matrixes that were not degassed shrunk considerably when dried since pores were formed by solvent displacement and entrapped air. At the low chitosan concentrations studied (2.3%, w/w), shrinking causes severe and irregular sample deformation. This may cause pores to collapse (see Figure 11).

Starch (Figure 10) and starch−chitosan-based scaffolds (Figure 15) show a similar morphology. As in chitosan-based samples, the pores are open, tubular, and orientated but the cell walls are thicker with regard to the chitosan scaffolds. The micropores of potato starch based foams frozen at −196 °C can be observed in Figure 9. A fairly homogeneous distribution of pore size (mean 2.5 μm ± 1.1) and shape is observed.

The differences observed in pore morphology and size between chitosan precipitated samples and SEPS samples might be due to the solvent phase (see Figures 14 and 12). During samples precipitation, the solvent surrounding the polymer molecules is in liquid phase and the solidification of chitosan is due to neutralization that takes place while the polymer chains are in solution, displaying enough freedom of movement to adopt different conformations. Conversely, when SEPS samples are formed, the chitosan solution is frozen (polymer and solvent in solid phase) so it would be expected that the polymer chains cannot alter their original conformation, therefore, producing a different structure. This may explain larger pores in SEPS samples.

Table 3. Overall Apparent Density and Porosity of Foams

specimen	composition	solid density (g cm^{-3})[a]	apparent density (ρ) (g cm^{-3})	calculated avg. porosity (%) (P from eq 1)
ST-P-20-15-SX	20% potato starch	1.472	0.425 ± 0.053	71.1%
ST-P-20-15/N-FD	20% potato starch	1.472	0.254 ± 0.011	82.7%
ST-P-20-N-FD	20% potato starch	1.472	0.195 ± 0.042	86.8%
ST-P20-N-SX	20% potato starch	1.472	0.661 ± 0.013	55.1%
ST-P-10-N-FD	10% potato starch	1.472	0.201 ± 0.012	86.4%
ST-SP-10-15-SX	10% sweet potato starch	1.500	0.178 ± 0.048	88.1%
ST-SP-10-15/N-FD	10% sweet potato starch	1.500	0.112 ± 0.016	92.6%
ST-SP-10-N-FD	10% sweet potato starch	1.500	0.111 ± 0.004	92.6%
ST-SP10-N-SX	10% sweet potato starch	1.500	0.458 ± 0.063	69.5%
ST-SP-20-N-FD	20% sweet potato starch	1.500	0.206 ± 0.018	86.3%
ST-C-10-15-SX	10% corn starch	1.450	0.235 ± 0.006	83.8%
ST-C-10-15/N-FD	10% corn starch	1.450	0.119 ± 0.056	91.8%
ST-C-10-N-FD	10% corn starch	1.450	0.831 ± 0.028	42.7%
ST-C-10-N-SX	10% corn starch	1.450	0.431 ± 0.016	70.3%
ST-C-20-N-FD	20% corn starch	1.450	0.241 ± 0.021	83.4%
CHS-N-DG	2.31% chitosan	1.426	0.114 ± 0.027	92.0%
CHS-15-DG	2.31% chitosan	1.426	0.199 ± 0.099	86.0%
CH-P-15-15	1% chitosan/15.8% potato starch	1.472	0.296 ± 0.048	79.9%

[a] See refs 60−63.

Table 4. Specimen Weights Before and after the SBF Immersion Tests

specimen	weight dry, before SBF (g)	weight soaked (SBF) (g)	weight soaked[a] (g)	weight dry, after SBF (g)
ST-C-10-15-S X	0.126	0.532	0.377	0.061
ST-P-20-15-S X	0.220	0.891	0.882	0.159
ST-SP-10-15-SX	0.120	0.213	0.052	0.092

[a] Soaked in deionized water.

3.2. Overall Apparent Density and Porosity. Overall apparent density and porosity values are listed in Table 3. Most porosity values are between 80% and 90% no mater the source or processing technique. The sweet potato based structures made by the freeze-drying technique (ST-SP-10-5/N-FD and ST-SP-10-N-FD) had the highest porosity (92.6%) and the lowest density (0.111 g/cm^3) while the corn starch based foam (ST-C-10-N-FD) had the lowest porosity (42.7%) and the highest density (0.831 g/cm^3).

3.3. SBF Tests. Table 4 shows starch-based specimen weights before and after the SBF immersion tests. For corn and potato starch foams, the weight of samples after immersion was about 4 times higher than the dry weight, while sweet potato starch absorbed less water than the others (the soaked weight was only about 2 times the dry weight).

Figures 16 and 17 show the topography of a corn-based scaffold after 21 days of immersion in SBF. Erosion caused a change in the structure of the foams but no bioactivity was detected since there was no formation of hydroxyapatite crystals on the surface of the foams, as expected. It is thus confirmed that for specific applications as bone tissue engineering scaffolds, the foams should be coated with a bioactive material (e.g., hydroxyapatite or bioactive glass).[54] Alternatively, composites containing bioactive inorganic particles can be fabricated.[2]

3.4. Indentation Tests. To assess the mechanical properties of the foams, indentation tests were performed. These types of tests provide information on the mechanical properties of porous structures such as the compressive collapse strength. Gibson and Ashby[55] have shown that, for foams with porosities values higher than 70%, the indentation pressure can be considered equal to the compressive plastic-collapse strength. This relation is expressed by eq 2,

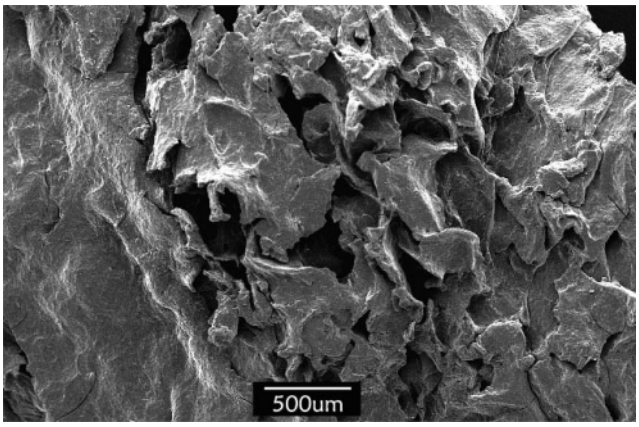

Figure 16. SEM micrograph of a corn starch scaffold frozen at −15 °C and produced by solvent exchange phase separation (SEPS) after 21 days in SBF showing signs of surface erosion but no formation of hydroxyapatite.

$$\sigma_{pl}^{*} \approx 0.3\sigma_{ys}\left(\frac{\rho}{\rho_o}\right)^{3/2} \quad (2)$$

where σ_{pl}^{*} is the compressive plastic-collapse strength, σ_{ys} is the yield strength of the solid material, and ρ/ρ_o is the relative density of the foam (apparent density divided by solid density).

The results of the indentation tests are shown in Table 5. Indentation pressure of chitosan SEPS samples are the lowest (0.19 and 0.42 MPa). This is due to the fact that the compressive plastic-collapse strength depends on relative density (see eq 2) and chitosan SEPS samples showed the lowest apparent density values which mean the lowest relative density values. Conversely, potato starch based scaffolds had the highest indentation pressure value (6.65 MPa) because of its high apparent density.

Potato starch based scaffolds processed by the TIPS technique at −196 °C showed a different result (1.65 MPa). Moreover, in

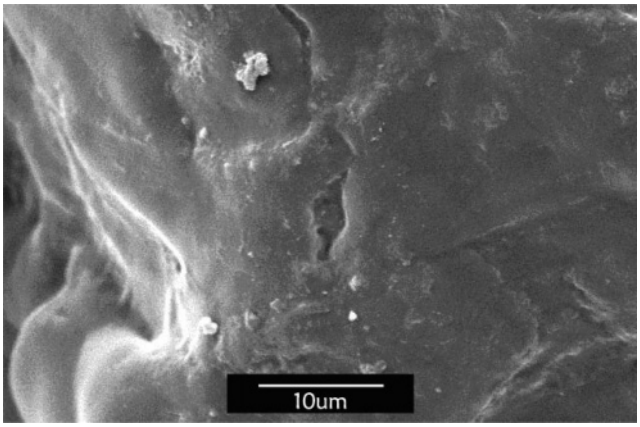

Figure 17. SEM micrograph showing the topography of a corn starch scaffold (SEPS) after 21 days in SBF showing signs of surface erosion but no formation of hydroxyapatite.

Table 5. Indentation Stress (MPa)

specimen	composition	indentation stress (MPa)	apparent density (ρ) (g cm^{-3})
ST-P-10-15-S X	10% potato starch	2.62 ± 0.44	0.173 ± 0.006
ST-P-20-15-S X	20% potato starch	6.65 ± 2.02	0.425 ± 0.053
ST-P-20-N-F D	20% potato starch	1.65 ± 0.05	0.195 ± 0.042
ST-SP-10-15-SX	10% sweet potato starch	3.08 ± 0.5	0.178 ± 0.048
ST-SP-20-N-F D	20% sweet potato starch	2.93 ± 0.13	0.206 ± 0.018
ST-C-10-15-S X	10% corn starch	2.52 ± 0.13	0.235 ± 0.006
ST-C-20-N-F D	20% corn starch	1.14 ± 0.11	0.241 ± 0.021
CHS-15-DG	2.31% chitosan	0.42 ± 0.13	0.199 ± 0.099
CHS-N-DG	2.31% chitosan	0.19 ± 0.12	0.114 ± 0.027
CH-P-15-15	1% chitosan/15.8% potato starch	2.05 ± 0.53	0.296 ± 0.048

all cases foams frozen at −196 °C had lower indentation values than foams frozen at −5 °C for the same starch source due to their morphology (micropores and thin cell walls).

Different techniques have been used elsewhere to assess mechanical properties of foams and several researchers have found a power-law relationship between compressive strength and foam density.[56,57] Nazarov et al.[58] reported compressive stress data of scaffolds of silk biomaterial matrixes fabricated by freeze-drying, salt leaching, and gas foaming. The values obtained by Nazarov for salt leaching and gas foaming scaffolds are similar to those of chitosan SEPS samples of the present study (0.28−0.175 MPa) but not as high as the values reached here by starch-based foams (6.65−1.14 MPa). However, blends of corn starch, ethylene vinyl alcohol, and cellulose acetate prepared by Gomes et al.[59] and processed by extrusion, compression molding, and solvent casting and particulate leaching have obtained higher compressive strengths (67.69−12.0 MPa) accompanied however by a low porosity (40−70%).

4. Conclusions

In the starch-based scaffolds production, both the solvent exchange phase separation (SEPS) and thermally induced phase separation (TIPS) methods are related to the physics of ice formation since pore size can be tailored by the freezing temperature of the starch paste. The microstructure of the foams depends on the structure of the ice crystals formed. High freezing rates produce thin or small crystals and, therefore, fine foam microstructures.

For chitosan-based foams, the pore size can be adjusted by choosing the most suitable processing technique. Macroporous foams are made with the SEPS technique whereas the production of precipitated chitosan pellets results in a microporous structure.

SBF tests were used to assess the biodegradation behavior of the scaffolds. Upon 21 days of immersion in SBF, no signs of bioactivity or formation of hydroxyapatite layers on scaffolds surfaces were observed, confirming that for applications in bone tissue engineering a combination of the present foams with bioactive phases, e.g., bioactive glass, will be required.

The indentation properties of the scaffolds depend on the foaming technique used (SEPS or TIPS) and on the source of the material (type of starch). Chitosan-based foams displayed the lowest stress values and SEPS potato starch foams the highest ones.

Acknowledgment. Financial support from the Royal Society for a visiting research fellowship for Dr. F. Torres at Imperial College is greatly appreciated. The authors would also like to thank Dr. Maria Elena López for experimental assistance in the indentation tests.

References and Notes

(1) Agrawal, C. M.; Ray, R. B. *J. Biomed. Mater. Res.* **2001**, *55*, 141.
(2) Boccaccini, A. R.; Maquet, V. *Compos. Sci. Technol.* **2003**, *63*, 2417.
(3) Reis, R. L. Polymers in Tissue engineering: Basic principles, main challenges and characterization requirements. Annual Technical Conference **2002**, *3*, 2680.
(4) Lu, L.; Mikos, A. G. *MRS Bull.* **1996**, *21*, 28.
(5) Boccaccini, A. R.; Maquet, V. *Compos. Sci. Technol.* **2003**, *63*, 2417.
(6) Gomes, M. E.; Godinho, J. S.; Tchalamov, D.; Cunha, A. M.; Reis, R. L. *Mater. Sci. Eng.* **2002**, *20*, 19.
(7) Leach, H. W. Gelatinization of starch. In *Starch: Chemistry and Technology. Vol. 1. Fundamental Aspects*; Whistler, R. L., Paschall, E. F., Eds.; Academic Press: New York, 1965; pp 289−307.
(8) Walter, W. M.; Truong, V. D.; Wiesenborn, D. P.; Carvajal, P. Rheological and Physicochemical Properties of Starches from Moist- and Dry-Type Sweetpotatoes. *J. Agric. Food Chem.* **2000**, *48*, 2937.
(9) Donald, A. M. *Rep. Prog. Phys.* **1994**, *57*, 1081.
(10) Hirano, S.; Seino, H.; Akiyama, Y.; Nonaka, I. *Polym. Mater. Sci. Eng.* **1988**, *59*, 897.
(11) Lee, K. Y.; Ha, W. S.; Park, W. H. *Biomaterials* **1995**, *16*, 1211.
(12) Vandevord, P. J.; Matthew, H. W. T.; Desilva, S. P.; Mayton, L.; Wu, B.; Wooley, P. H. *J. Biomed. Mater. Res.* **2002**, *59*, 585.
(13) Koide, S. S. *Nutr. Res.* **1998**, *18*, 1091.
(14) Nordtveit, R. J.; Varum, K. M.; Smidsrod, O. *Carbohydr. Polym.* **1994**, *23*, 253.
(15) Sashiwa, H.; Saito, K.; Saimota, H.; Minami, S.; Okamoto, Y.; Matsuhashi, A.; Shigemasa, Y. In *Chitin enzymology*; Muzzarelli, R. A. A., Ed.; European Chitin Society: Ancona, 1993; pp 177−186.
(16) Di Martino, A.; Sittinger, M.; Risbud, M. V. *Biomaterials* **2005**, *26*, 5983.
(17) Tuzlakoglu, K.; Alves, C. M.; Mano, J. F.; Reis, R. L. *Macromol. Biosci.* **2004**, *4*, 811.
(18) Mao, J.; Zhao, L.; De, Y. K.; Shang, Q.; Yang, G.; Cao, Y. *J. Biomed. Mater. Res. A* **2003**, *64*, 301.
(19) Mao, J. S.; Zhao, L. G.; Yin, Y. J.; Yao, K. D. *Biomaterials* **2003**, *24*, 1067.
(20) Xia, W.; Liu, W.; Cui, L.; Liu, Y.; Zhong, W.; Liu, D.; Wu, J.; Chua, K.; Cao, Y. *J. Biomed. Mater. Res., Part B* **2004**, *71*, 373.
(21) Iwasaki, N.; Yamane, S.; Majima, T.; Kasahara, Y.; Minami, A.; Harada, K.; Nonaka, S.; Maekawa, N.; Tamura, H.; Tokura, S.; Shiono, M.; Monde, K.; Nishimura, S. *Biomacromolecules* **2004**, *5*, 828.
(22) Li, Z.; Ramay, H. R.; Hauch, K. D.; Xiao, D.; Zhang, M. *Biomaterials* **2005**, *26*, 3919.
(23) Ma, L.; Gao, C.; Mao, Z.; Zhou, J.; Shen, J.; Hu, X.; Han, C. *Biomaterials* **2003**, *24*, 4833.
(24) Li, X.; Feng, Q.; Jiao, Y.; Cui, F. *Polym. Int.* **2005**, *54*, 1034.
(25) Zhang, Y.; Zhang, M. *J. Biomed. Mater. Res.* **2001**, *55*, 304.

(26) Yin, Y.; Ye, F.; Cui, J.; Zhang, F.; Li, X.; Yao, K. *J. Biomed. Mater. Res., Part A* **2003**, *67*, 844.
(27) Yamane, S.; Iwasaki, N.; Majima, T.; Funakoshi, T.; Masuko, T.; Harada, K.; Minami, A.; Monde, K.; Nishimura, S. *Biomaterials* **2005**, *26*, 611.
(28) Masuko, T.; Iwasaki, N.; Yamane, S.; Funakoshi, T.; Majima, T.; Minami, A.; Ohsuga, N.; Ohta, T.; Nishimura, S. *Biomaterials* **2005**, *26*, 5339.
(29) Baran, E. T.; Tuzlakoglu, K.; Salgado, A. J.; Reis, R. L. *J. Mater. Sci.: Mater. Med.* **2004**, *15*, 161.
(30) Mwale, F.; Iordanova, M.; Demers, C. N.; Steffen, T.; Roughley, P.; Antoniou, J. *Tissue Eng.* **2005**, *11*, 130.
(31) Sugimoto, M.; Morimoto, M.; Sashiwa, H.; Saimoto, H.; Shigemasa, Y. *Carbohydr. Polym.* **1998**, *36*, 49.
(32) Chow, K. S.; Khor, E. *Biomacromolecules* **2000**, *1*, 61.
(33) Fernandez-Cervera, M.; Heinamaki, J.; Krogars, K.; Jorgensen, A. C.; Korjalaimen, M.; Iraizoz-Colarte, A.; Yliruusi, J. *AAPS Pharm. Sci. Technol.* **2004**, *5*, Article 15.
(34) Arvanitoyannis, I.; Nakayama, I.; Aiba, S. *Carbohydr. Polym.* **1998**, *37*, 371.
(35) Budtova, T.; Belnikevich, N.; Kalyuzhnaya, L.; Alexeev, V.; Bronnikov, S.; Vesnebolotskaya, S.; Zoolshoev, Z. *J. Appl. Polym. Sci.* **2002**, *84*, 1114.
(36) Muzzarelli, R. A. A.; Rochetti, R.; Stanic, V.; Weckx, M. In *Chitin Handbook*; Muzzarelli, R. A. A., Peter, M. G., Eds.; European Chitin Society: Grottammare, 1997; pp 109−117.
(37) Wang, W.; Bo, S.; Li, S.; Quin, W. *Int. J. Biol. Macromol.* **1991**, *13*, 281.
(38) Swinkels, J. J. M. Sources of starch, its chemistry and physics. In *Starch Conversion Technology*; Van Beynum, G. M. A., Roels, J. A., Eds.; Marcel Dekker Inc.: New York, 1985.
(39) Stepto, R. F. T. *Macromol. Symp.* **2003**, *201*, 203.
(40) Souza, R. C. R.; Andrade, C. T. *Adv. Polym. Technol.* **2002**, *21*, 17.
(41) Guan, J.; Hanna, M. A. *Biomacromolecules* **2004**, *5*, 2329.
(42) Torres, F. G.; Díaz, R. *Polym. Polym. Compos.* **2004**, *12*, 705.
(43) Haritos, G. K.; Hager, J. W.; Amos, A. K.; Salkind, M. J.; Wang, A. S. D. *Int. J. Solids Struct.* **1988**, *24*, 1081.
(44) Safinia, L.; Mantalaris, A.; Bismarck, A. *Langmuir* **2006**, *22*, 3235.
(45) Malafaya, P. B.; Elvira, C.; Gallardo, A.; San Román, J.; Reis, R. L. Porous starch-based drug delivery systems processed by a microwave route. *J. Biomater. Sci. Polym.* **2001**, *12*, 1227.
(46) Korhonen, O.; Pohja, S.; Peltonen, S.; Suihko, E.; Vidgren, M.; Paronen, P.; Ketolainen, J. *AAPS Pharm. Sci. Technol.* **2002**, *3*, 34.
(47) ASTM F2450-04. Standard Guide for Assessing Microstructure of Polymeric Scaffolds for Use in Tissue Engineered Medical Products.
(48) Kokubo, T.; Kushitani, H.; Sakka, S.; Kitsugi, T.; Yamamuro, T. *J. Biomed. Mater. Res.* **1990**, *24*, 721.
(49) ASTM D2240. Standard Test Method for Rubber Property−Durometer Hardness.
(50) Donovan, J. W. *Biopolymers* **1979**, *18*, 263.
(51) Slade, L.; Levine, H. *Crit. Rev. Food Sci. Nutr.* **1991**, *30*, 115.
(52) Tananuwong, K.; Reid, D. *J. Agric. Food Chem.* **2004**, *52*, 4308.
(53) Deville, S.; Saiz, E.; Nalla, R. K. *Science* **2006**, *311*, 515.
(54) Roether, J. A.; Boccaccini, A. R.; Hench, L. L.; Maquet, V.; Gautier, S.; Jérôme, R. *Biomaterials* **2002**, *23*, 3871.
(55) Gibson, L. J.; Ashby, M. F. *Cellular solids: Structure & properties*; Cambridge University Press: Cambridge, 1997.
(56) Hutchinson, R. J.; Siodlak, G. D. E.; Smith, A. C. *J. Mater. Sci.* **1987**, *22*, 3956.
(57) Willett, J. L.; Shongren, R. L. *Polymer* **2002**, *43*, 5935.
(58) Nazarov, R.; Hyoung-Joon, J.; Kaplan, D. L. *Biomacromolecules* **2004**, *5*, 718.
(59) Gomes, M. E.; Godinho, J. S.; Tchalamov, D.; Cunha, A. M.; Reis, R. L. *Mater. Sci. Eng. C* **2002**, *20*, 19.
(60) Nelson, S. O.; Lawrence, K. C.; Prakash, A. *J. Microwave Power* **1991**, *26*, 178.
(61) Maroulis, Z. B.; Shah, K.; Saravacos, G. D. *J. Food Sci.* **1991**, *56*, 773.
(62) Wang, L. J.; Ganjyal, G. M.; Jones, D. D.; Weller, C. L.; Hanna, M. A. *Adv. Polym. Technol.* **2005**, *24*, 29.
(63) Fernández Cervera, M.; Heinämäki, J.; Räsänen, M.; Maunu, S. L.; Karjalainen, M.; Nieto Acosta, O. M.; Iraizoz Colarte, A.; Yliruusi, J. *Carbohydr. Polym.* **2004**, *58*, 401.

BM0605311